Advances in Colloid and Interface Science 305 (2022) 102688

Contents lists available at ScienceDirect

Advances in Colloid and Interface Science

journal homepage: www.elsevier.com/locate/cis

Advances in antibubble formation and potential applications

Rabia Zia [a], Akmal Nazir [b,*], Albert T. Poortinga [c], Cornelus F. van Nostrum [a,*]

[a] Department of Pharmaceutics, Utrecht Institute for Pharmaceutical Sciences, Utrecht University, Utrecht, the Netherlands
[b] Department of Food Science, College of Agriculture and Veterinary Medicine, United Arab Emirates University, Al Ain, United Arab Emirates
[c] Department of Mechanical Engineering, Polymer Technology, Eindhoven University of Technology, Eindhoven, the Netherlands

ARTICLE INFO

Keywords:
Antibubble
Bubble
Liquid marble
Pickering emulsion
Air-liquid interface
Stability

ABSTRACT

Antibubbles are unusual physical objects consisting of a liquid core(s) surrounded by a thin air film/shell while in a bulk liquid. Antibubbles carry two air-liquid interfaces, i.e., one with the inner liquid and the other with the outer liquid. The distinct structure of antibubbles makes them quite attractive for drug and therapeutic delivery, although their potential applications have not been realized so far. The major challenge in this regard is a short-lived span of antibubbles, which is usually in the order of a few minutes to a few hours based on the stabilization mechanism used. We present a critical overview of different techniques that can be used to generate antibubbles. This includes a more commonly applied conventional approach in which the air-film is created through surface entrapment when a liquid jet/drop falls on a bulk liquid. The other available options rely on entirely different mechanisms for antibubble formation, for instance, through drop encapsulation by a submerged air bubble, or through evaporation/sublimation of volatile oil from a W/O/W double emulsion. Furthermore, the mechanisms of antibubble formation and collapse, and the factors affecting their stability have been discussed explicitly; and wherever required, the concept is correlated to other allied physical objects such as bubbles, liquid marbles, etc. Finally, the potential applications, research gaps in the existing knowledge, and some directions for future research are provided towards the end of this article.

1. Introduction

Antibubbles have a discrete air film separating the inner liquid core from an outer bulk liquid, i.e., a water-in-air-in-water structure (Fig. 1). Hughes and Hughes [1] were the first to report the existence of such unusual physical objects. Initially, they were assigned different names, such as inverted or inverse bubbles [2,3], and finally, they were given the name antibubbles in 1974 [4]. Although antibubbles were discovered a long time ago, they attracted the attention of the scientific community since the beginning of this century through the use of high-speed imaging. Most of the studies in the past two decades were focused on understanding the mechanisms of antibubble formation and collapse [5–8], and the factors affecting their stability [9–13]. Antibubbles can be produced simply by pouring a suitable liquid mixture (e.g., an aqueous detergent solution) at the surface of the same mixture [5]. The falling liquid thus entraps a thin air film, leading to antibubble formation. The previously conducted fundamental investigations on antibubbles usually adopted this classical approach of antibubble formation. Besides, the antibubble formation can also be realized through some modifications of this classical technique [14,15], or through entirely different approaches, e.g., coalescence of microbubbles [16,17], submerged drop encapsulation [18], and Pickering stabilization [19,20].

The significance of antibubbles lies in the existence of a distinct structure that promises unique applications as encapsulation matrices. For instance, the entrapment of the liquid core by an air-shell minimizes chances of release of the encapsulated compound by diffusion or any possible interaction with the surroundings, which is usually the case with conventional encapsulation matrices. Furthermore, they can be used for a more precise and a site-specific delivery, e.g., through ultrasounds or magnetic fields [17,21]. Keeping in view the capability of antibubbles for encapsulation, delivery and controlled release of drugs and bioactive compounds, the present article has been written with an aim to comprehensively analyze the existing literature. We have critically discussed different production methods and related process parameters. The role of surfactants and allied factors on the stability of antibubbles is also presented, with a special emphasis on particle-based stabilization as the most viable option to achieve extended antibubble lifetime. More importantly, the potential applications, research gaps in the existing knowledge, and some directions for the future research is provided towards the end of this article.

* Corresponding authors.
E-mail addresses: akmal.nazir@uaeu.ac.ae (A. Nazir), C.F.vanNostrum@uu.nl (C.F. van Nostrum).

https://doi.org/10.1016/j.cis.2022.102688
Received in revised form 25 April 2022;
Available online 30 April 2022

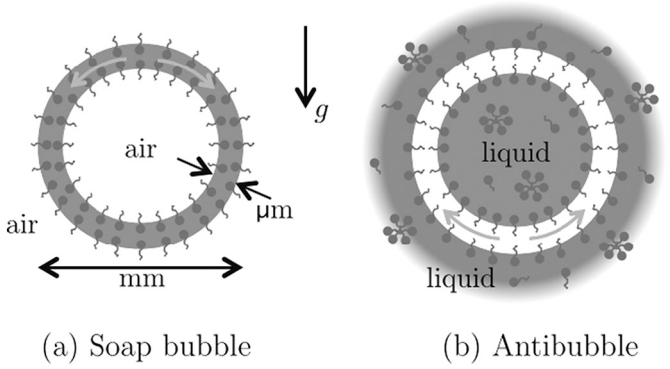

Fig. 1. A schematic representation of a soap bubble and antibubble. The hydrophilic heads and hydrophobic tails of surfactant molecules (in green) are facing towards liquid and air, respectively. The drainage of liquid film (in case of bubble) and air film (in case of antibubble), under gravity (g) is represented by orange arrows [13].

2. Techniques for the preparation of antibubbles

In this section we will discuss the different techniques available to produce antibubbles. These techniques are summarized in Table 1.

2.1. Conventional or falling liquid method

Initially, antibubbles were prepared by using a simple experimental setup, which still seems to dominate in more recent studies. This conventional method constitutes dropping a liquid (in the form of a jet or a drop) from a certain height into a tank with greater volume of the same liquid. When the falling liquid touches the bulk liquid below it sinks down due to its momentum entrapping a gas film between the external liquid and the falling liquid, creating a non-wetting situation, which results in creation of an antibubble. This simple methodology only requires two main components: i) a capillary or a dropper to throw a liquid from the top, and ii) a container, cell, or tank with a larger quantity of liquid. In an earlier study conducted by Dorobolo et al. [5], antibubbles were produced with a simple experimental setup using an aqueous solution of dishwashing soap. A beaker was used to drop the liquid into an open reservoir filled with the same liquid mixture. In such arrangement, the liquid from the beaker flows down in continuous fashion to form a jet, and enters in bulk liquid while entrapping thin air film. Consequently, Rayleigh plateau instabilities will cause the jet to break into multiple droplets covered with thin air film, i.e. the antibubbles are formed (Fig. 2a). The continuous flow of the falling liquid pushes the newly formed antibubbles further down in the bulk liquid. Notably, the liquid jet can also be developed in a more controlled fashion, e.g., as reported in [6,9]. A further advanced and more sophisticated apparatus (using the same approach) was recently reported by Vitry et al. [13]. A gas bell was used inside the reservoir to supply a controlled air quality to the falling liquid jet, i.e., for the antibubble formation. The flow of the liquid (jet) and the gas inside the immersed bell was carefully regulated by a pressure controller. This apparatus provided a good control on various process parameters for antibubble formation. However, the drawback of dropping the liquid in the form of a jet is that it has less control on droplet size being formed by Rayleigh instabilities. Therefore, Kim and Stone [10] came up with a modified apparatus in which the liquid from the reservoir (a plexiglass vessel) was continuously drawn (using a pump) and then injected drop by drop (diameter ≈ 6 mm) into the reservoir through a pipe (diameter = 5 mm) at a certain height above liquid pool. The apparatus was also provided with a filter for drainage of any foam that can possible hinder antibubble formation. This apparatus provided an effective control on the falling drop height, size, and speed. As reported by the authors, the successful formation of an antibubble in this case requires two main steps: i) formation of a liquid cavity while entrapping an air film, and ii) pinching of the liquid-air cavity resulting in antibubble formation (Fig. 2b). However, there could be two unfavorable situations that can hinder antibubble formation: i) a sufficient air film development but lack of pinching at the back, or ii) an improper air film formation due to a rapid drainage of the air. Here, the inertia of penetrating liquid column together with viscous thinning of air film controls the first step in the formation of antibubbles, while pinching of the liquid column (and thus detachment of the antibubble) is driven by surface tension.

In the past three decades, the phenomena of drop impact on liquid surface attracted attention of many physicists [22–36]; however, only few studies are available on the formation of antibubble from a single drop while impacting on a bulk liquid surface. The formation of an antibubble from a successful collision between falling drop and bulk liquid surface requires a careful optimization of different parameters, such as height (h_d), velocity (u) and radius (R_d) of the falling drop, which are strongly correlated to each other [10]. The falling drop should have a minimum speed in order accomplish the first step, i.e., cavity formation, as mentioned above paragraph. Kim and Stone [10] related this with critical Weber number $\rho u^2 R_d/\gamma > 1$, where ρ and γ are density and surface tension of the liquid. Based on this, the critical velocity (u_c) was reported as $u_c > (\gamma/\rho R_d)^{0.5}$, which shows its dependency on the drop radius apart from liquid properties (see Table 1 for optimum conditions to produce an antibubble of 2.2 mm radius).

The cavity formation upon collision between drop and liquid surface is a consequence of conversion of drop kinetic energy into surface energy [37]. Therefore, low-velocity drop impacts, such as floating and bouncing [34–36,38–40], do not lead to antibubble formation. Recently, Wang et al. [41] performed an experimental study on antibubble formation by a single drop impact, i.e., similar to Kim & Stone [10], using a high quality imaging. The primary difference in the experimental setups of the two studies is that Wang and co-workers used much larger falling drop height (probably due to the reason that the drops had zero initial velocity), which was not the case in the other study. Wang et al. [41] studied falling drop dynamics and identified different regimes based on drop impact velocity or kinetic energy. As presented by the authors, the drop collision on bulk liquid leads to splashing, cavity formation, and then rise of a thick jet on the liquid surface (Fig. 3). The impact velocity determines height of the rising jet which in turn leads to different regimes, i.e. no droplet, single droplet, double droplet, and antibubble formation, each separated by a threshold kinetic energy of the falling drop (Fig. 4). Only the double droplet regime is relevant to antibubble formation and is therefore presented here. The thick jet (having a sufficient height) breaks into two droplets: primary and secondary (Figs. 3, 76 ms – 92 ms). Subsequently, the primary droplet collides with the secondary droplet and pushes it into the bulk liquid, which forms an antibubble (Figs. 3, 1100 ms). Whereas, the primary droplet remains on the surface for a while, and then coalesces with the bulk liquid (Fig. 3, 258 ms). Here it should be noted that contrary to Wang et al. [41], Kim & Stone [10] did not report similar regimes; mainly due to the reason that in their study falling drops were elongated (Fig. 2b). Hence, shape of the impinging drop is also a key parameter that can produce different impact dynamics, and so can also influence antibubble formation.

Additionally, physical properties of the liquid such as surface tension and viscosity are also critical to the formation of antibubbles (either through a falling jet or drop method). The presence of a surface-active agent is crucial for the formation as well as the stability of antibubbles (as in some cases the antibubbles may develop without surfactants but

Table 1
A comparison between different techniques used for antibubble formation.

Description of process/apparatus (Φ = nozzle inner diameter; h = drop falling height; u = drop velocity; Q = flow rate)	Mixture composition and stabilization mechanism	Characteristics of antibubbles (d = diameter; r = radius; x = air-film thickness)	Lifetime	Ref.
i) Falling liquid jet				
Pouring liquid mixture via beaker into a bulk liquid surface.	Aqueous solution containing commercial dishwashing detergent (0.1%).	d = 5–16 mm x = 3 μm	2 min	[5,68]
A controlled pouring of liquid mixture via a nozzle on a bulk liquid surface (h = 5 mm).	Aqueous solution of $C_{12}E_6$ (10^{-3} M), glycerol in bulk solution to adjust density.	r = 5–15 mm x = 3 μm	4 min	[6]
A controlled pouring of liquid mixture via a nozzle on a bulk liquid surface (Φ = 4 mm; h = 1 cm; u = 1 cm/s).	Aqueous solution of commercial dishwashing detergent (0.8%).	r = 3–13 mm x = 0.2–1.0 μm	1–7 min	[9]
Pouring liquid mixture via beaker into a bulk liquid.	Aqueous solution containing different surfactants: commercial dishwashing detergent (0.6%) with or without glycerol (25%), sodium lauryl-dioxyethylene sulfate, cocoamidopropyl betaine, or myristic acid.	d = 10 ± 5 μm	2–4 min	[11]
Pouring liquid mixture via a nozzle on a bulk liquid surface (Φ = 0.7 mm or 1.6 mm; h = 2 cm).	Aqueous solution of different surfactants: $C_{12}E_6$, and Triton X-100, with or without glycerol.	r = 0.5–2.5 mm @ 0.7 mm nozzle r = 1–4 mm @ 1.6 mm nozzle x = 4.0 ± 1.4 μm	0.5–2.5 min	[13]
ii) Falling liquid drop				
The liquid drops emerging from a nozzle fall on bulk liquid surface (Φ = 2 mm; h = 1–20 mm; u = 6–29 cm/s).	An aqueous solution of commercial dishwashing detergent (0.1%).	r = 1.5–2.5 mm Optimum conditions for an antibubble of 2.2 mm radius: h = 11 mm, and u < 24 cm/s.	–	[10]
The liquid drops emerging from a syringe fall on a bulk liquid surface (h = 0–60 cm; u = 0–3.2 m/s).	An aqueous solution of commercial dishwashing detergent (1%).	d = 2–3 mm x = 5–20 μm	0.3–1 min	[41]
iii) Foam layer or liquid film (multilayered antibubbles)				
The liquid drops emerging from a nozzle first fall on liquid film/foam layer and then on bulk liquid surface (Φ = 0.8–1.6 mm; u = 1.1 m/s).	An aqueous solution of linear alkylbenzenesulfonate.	d = 3.3–4.6 mm x = 8.3–35 μm	–	[14]
iv) Falling drop pairs				
The liquid drops emerging from a syringe fall on a bulk liquid surface in pairs (u = 0.5–20 m/s).	Aqueous solution of Triton X-100 (1%).	d = ~0.5–3.0 mm	–	[15]
v) Microbubble coalescence				
The microbubbles were generated through a submerged nozzle in upward direction (Φ = 0.78 mm; Q = 210 ml/min).	An aqueous solution with glycerol (0–80%)	d = up to 5 mm	1 min - 1 h.	[16]
vi) Submerged drop encapsulation				
Taylor flow (i.e., gas-liquid mixture) injection in bulk liquid through submerged microchannel in upward direction (Φ = 0.3–1 mm; Q_{gas} = 10–80 ml/min; Q_{liquid} = 3–20 ml/min).	An aqueous solution with glycerol (0–70%)	d = ~3 mm	–	[18]
vii) Falling liquid marble				
The drops of a liquid mixture were formed through a syringe, coated with silica particles, gelled (by cooling) to form liquid marbles, and then dropped on a bulk liquid (h = 4 cm).	Liquid drop/marble: 30% maltodextrin 33 DE and 2.5% gelatin in water. Particles used for coating liquid marbles: hydrophobized H18 fumed silica particles. Bulk liquid: An aqueous solution containing 1% H30 fumed silica particles, 1% NaCl and 10% sucrose.	d = ~ 2.5 mm x = 30 μm	> 20 h	[19]
viii) Pickering double emulsion				
Formation of Pickering double emulsion ($W_1/O/W_2$) using aqueous phases with glass-forming solute and volatile oil, followed by freeze drying (to evaporate water and oil) and rehydration to produce antibubbles.	W_1: 25% maltodextrin 33DE O: Hexane + HDK H18 silica nanoparticle (2.5%) W_2: 25% maltodextrin 33DE + HDK H30 silica nanoparticles (0.5%)	d = 10–60 μm, approx.	Stable for at least several hours.	[20] Other related articles: [49,67]

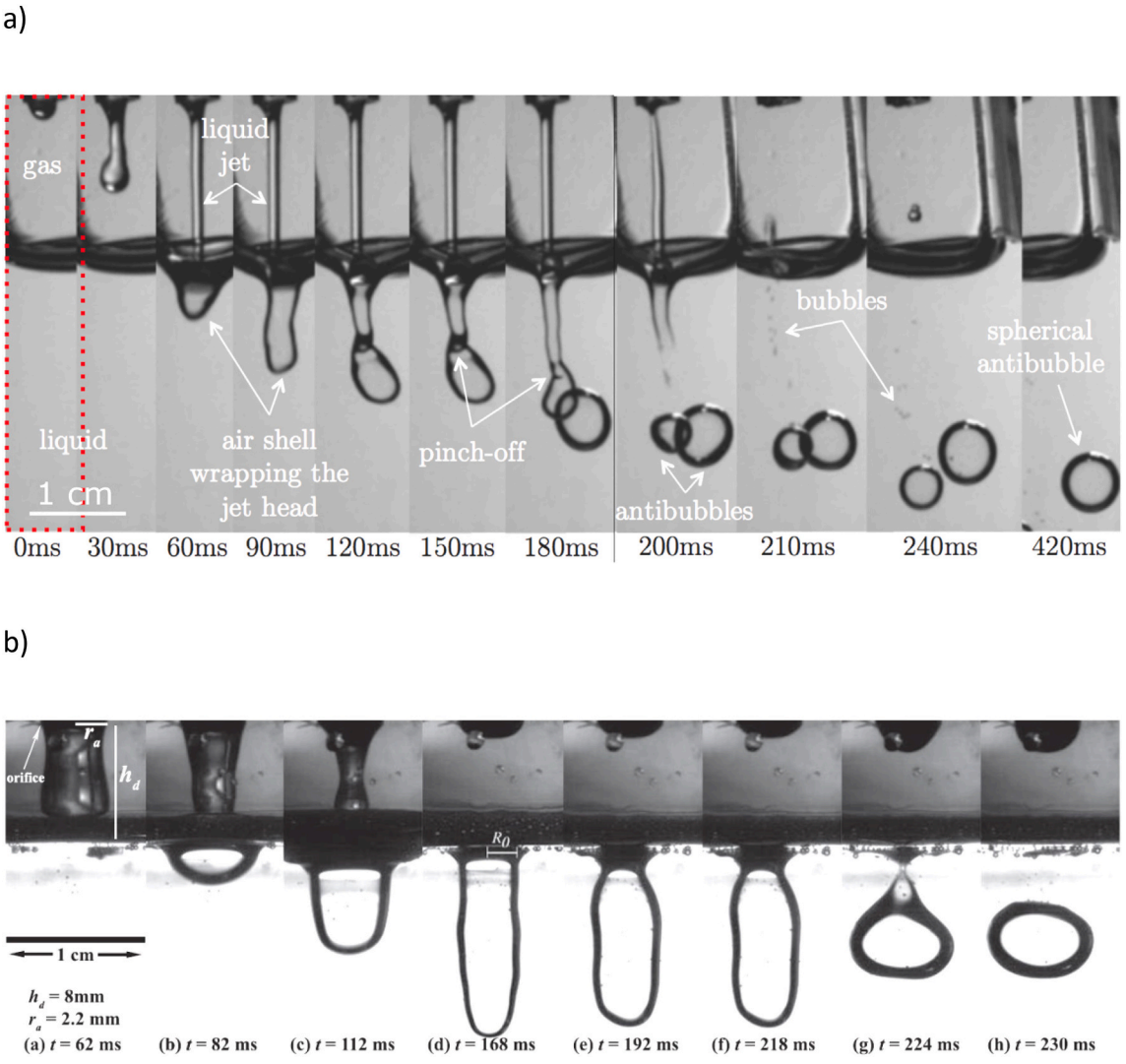

Fig. 2. Formation of antibubbles by a falling (a) jet [13], or (b) drop [10]. The black boundary represents thin air film.

they will be very short lived). The surfactants help in lowering of the interfacial tension and allow the air film to sustain. Commercial soaps and various anionic and non-ionic surfactants have been reported in different studies on antibubble formation (Table 1).

As apparent from earlier investigations, the antibubbles can be formed without any adjustment of the viscosity of either falling liquid or bulk liquid, i.e., an aqueous solution of a suitable surfactant can easily result in antibubble formation [5,10]. But this requires optimal adjustment of other parameters (discussed above) to allow air-film entrapment and pinch-off phenomena. However, the viscosity of the falling liquid relative to the viscosity of bulk liquid may have different implications. For instance, if we consider penetration of falling liquid into the bulk liquid (an important step in antibubble formation), a higher viscosity of the falling liquid leads to a higher chance of antibubble formation than the other way around [42]. Furthermore, a viscous drop can effectively maintain a stable air film that can nicely wrap around the entire drop to generate an antibubble. On the other hand, a higher viscosity of the bulk liquid usually requires more impact energy for cavity formation. However, once an antibubble is formed, a more viscous bulk liquid can promise an extended lifetime by damping incoming capillary waves [11]. These capillary waves are generated at the surface of newly born antibubble by a sudden change of topology due to air-film pinch off. Hence, from this discussion we can conclude that in this method a difference in viscosities between falling liquid and bulk liquid is always favorable, either through facilitating lubrication process for air-film entrapment or through damping of the capillary waves.

2.2. *Antibubble formation through foam layer or liquid film*

This approach is quite similar to the falling drop method; however, in this case the drop first falls on a foam layer (laid on bulk liquid surface) or liquid film (held above bulk liquid surface) before it strikes at the bulk liquid [14]. As soon as the droplet touches the foam layer, the liquid film is stretched and a cavity is created on the foam surface (Fig. 5a). The liquid drop traps the air layer, and moves downward under the effect of gravity. Thus, the droplet is already surrounded by gas and liquid films,

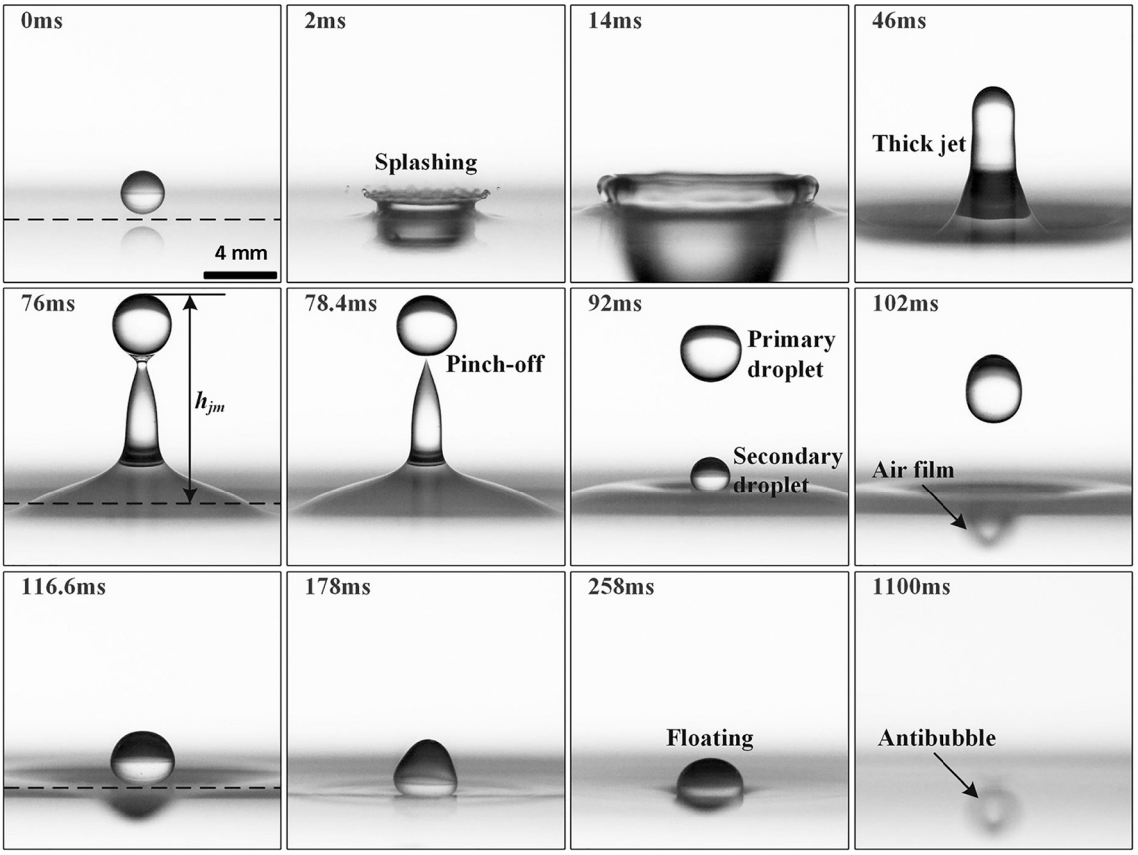

Fig. 3. Antibubble formation via a drop impact on bulk liquid surface [41].

which then enters into the bulk liquid and creates an antibubble. In a similar way, the antibubbles can be created through a liquid film held above the bulk liquid surface. When a droplet hits a liquid film, it wraps the liquid film due to surface tension while leaving a gas layer between the droplet and liquid film. Hence, an antibubble is already formed before the droplet touches the bulk liquid. When the antibubble strikes the bulk liquid surface, another gas film is entrapped but at the same time the middle liquid film will merge with the external bulk liquid, leaving behind a regular antibubble (single layered antibubble) in the bulk solution. Through this approach, a multilayered antibubble can also be produced when a liquid droplet is passed through several liquid layers and finally through a foam layer before entering into the bulk liquid (Fig. 5b). The antibubble formation through foam layer or liquid films seems quite fascinating, however, to the best of our knowledge, this is the only study in which the antibubbles were produced through such arrangements.

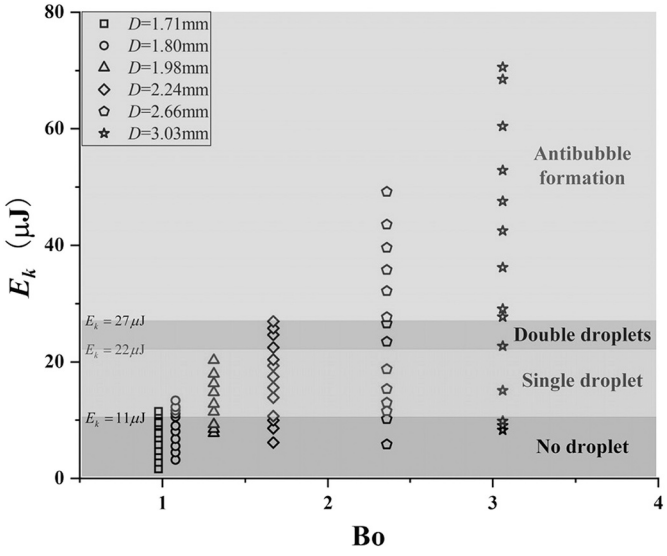

Fig. 4. Classification of drop impact phenomena into different regimes as a function of drop kinetic energy, E_k. Bond number, Bo, represents the ratio between the gravitational and surface forces, i.e., Bo $= 4\rho g R_d^2/\gamma$ [41].

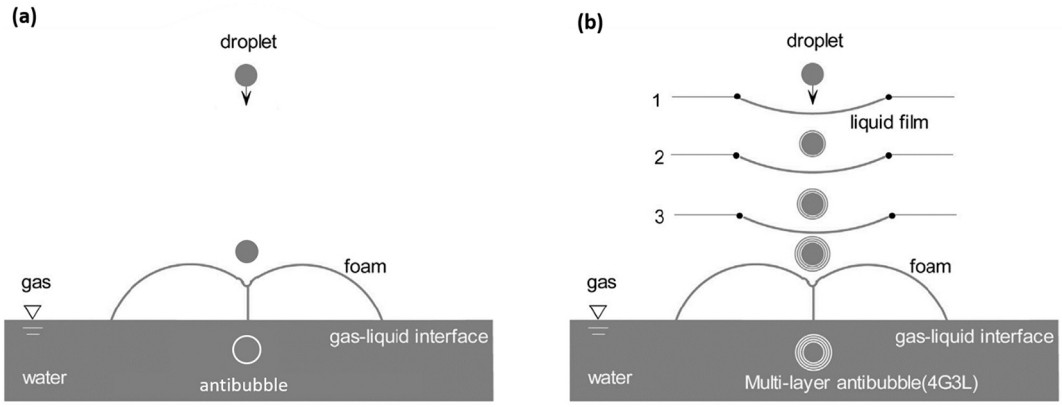

Fig. 5. A schematic representation of single-layered (a) and multilayered (b) antibubble formation using foam layer or liquid films [14].

2.3. *Antibubble formation through falling drop pairs*

In an attempt to further increase the probability of antibubble formation, Song and coworkers [15] reported a modified approach for antibubble formation through successive impinging of falling drop pairs, rather similar to Wang et al. [41]. In this case, the first drop will coalesce with the bulk liquid surface and creates a cavity (a crater-like surface deformation). The second drop then impinges into this cavity, entraps thin air film, and finally pinches off to give rise to an antibubble (Fig. 6a). The impact of a liquid drop on bulk liquid surface is usually categorized into four different regimes: low-energy coalescence, bouncing, high-energy coalescence, and jetting or splashing. The high-

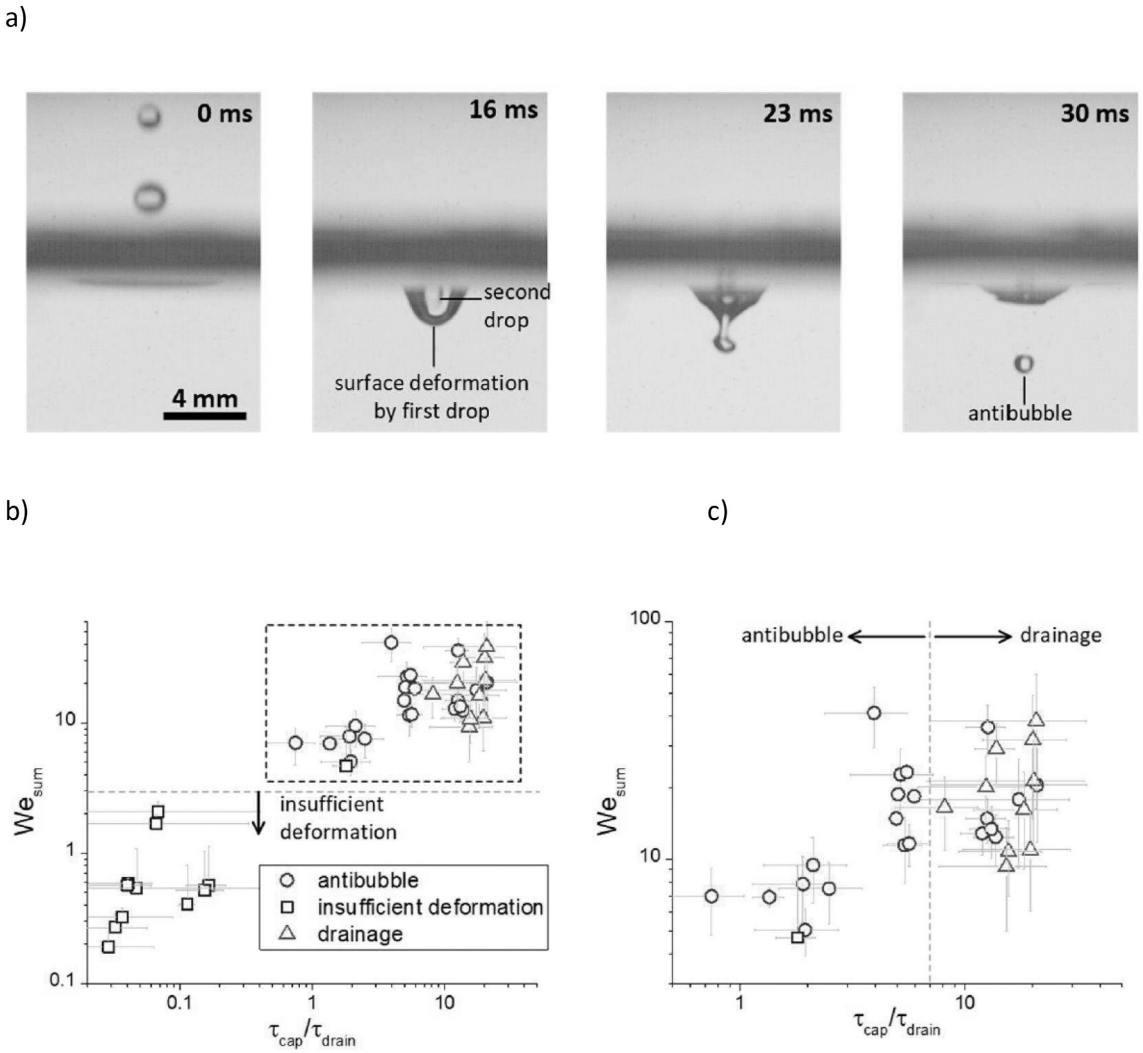

Fig. 6. a) Different stages of antibubble formation through falling drop pair, b) a relation between summative Weber number (We_{sum}) and ratio of bubble pinch-off time to air-film drainage time (τ_{cap}/τ_{drain}), and c) is magnified view of dashed box in b [15].

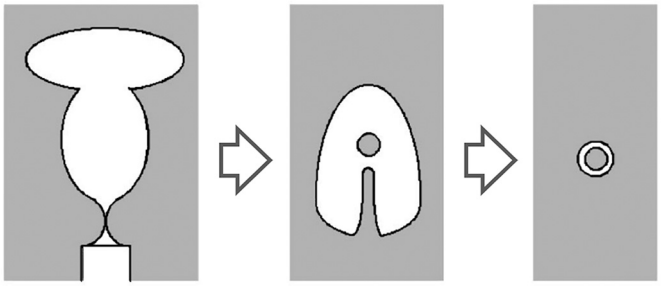

Fig. 7. Formation of an antibubble due to coalescence between two consecutive bubbles emerging through a submerged nozzle [16].

energy coalescence is the most practically feasible regime for antibubble formation through a falling drop pair [15]. The condition for a crater-like surface deformation for a high-energy coalescence can be described through the Weber number ($We = \rho u^2 D_d/\gamma$) and Ohnesorge number ($Oh = \mu/\sqrt{\rho\gamma D_d}$) of the falling drop as [43,44]:

$$We \bullet Oh^{-0.58} > 119 \quad (1)$$

where, μ, ρ and γ are viscosity, density and surface tension of liquid mixture, respectively, and u and D_d are velocity and diameter of the falling drop, respectively. Once the bulk liquid surface has reached to its maximum deformation (becoming stagnant for a while) in response to the first impact, it represents an optimal instant (Δt_{opt}) for a subsequent impact. For an optimal delay between successive impacts (i.e., $\Delta t \approx \Delta t_{opt}$), the authors came up with two additional criteria for a successful antibubble formation, i.e., $We_{sum} > 3$ and $\tau_{cap}/\tau_{drain} < 7$, where We_{sum} is summative Weber number of two drops, whereas τ_{cap} and τ_{drain} are bubble pinch-off and air-film drainage timescales (Fig. 6b&c).

2.4. Antibubble formation through coalescence of microbubbles

A more complex process than the classical approach of antibubble formation involves coalescence of two microbubbles in a viscous liquid [16]. Principally, a collision between two parent microbubbles (generated via a submerged nozzle) causes a rapid inrush of liquid giving rise to a Rayleigh jet. The interfacial instabilities, which operate together with this infolding process, eventually break the interface and give rise to a drop inside the coalesced bubble. Hence, under ideal conditions, successive bubbling (through the submerged needle) and inverted dripping (i.e., drop entrapment) processes will form antibubbles (Fig. 7). Notably, a successful drop entrapment is an interplay of inertial, viscous, and capillary forces, which in turn are affected by various fluidic (mainly liquid viscosity and bubbling frequency) and geometric (nozzle size and liquid column height) properties. A liquid viscosity of 14.5 cP (an aqueous solution containing 66% glycerol) and a bubbling frequency of 50 bubbles per second were found optimum for antibubbles formation [16]. Furthermore, the frequency of drop entrapment was higher when the coalescence occurred close to the needle, greatly attributed to the localized chaotic regime when the lower bubble is detached from nozzle.

A similar approach was used by Postema et al. [17] who produced micron-sized antibubbles through ultrasound-induced coalescence of microbubbles. They reported coalescence of a large air microbubble (30 μm, unencapsulated) and a small air microbubble (7.5 μm, encapsulated in human serum albumin) through application of 0.5 MHz ultrasounds at 0.8 MPa peak-negative acoustic pressure. The coalescence starts with instability of the larger bubble's surface close to the smaller bubble. This will further result in liquid jet formation followed by a drop pinch-off in the larger bubble, and finally, an antibubble will be produced. To the best of our knowledge, this is the only study on the formation of antibubbles via ultrasound-based coalescence of microbubbles. However, a further investigation is needed to explain effects of various process parameters on antibubble formation.

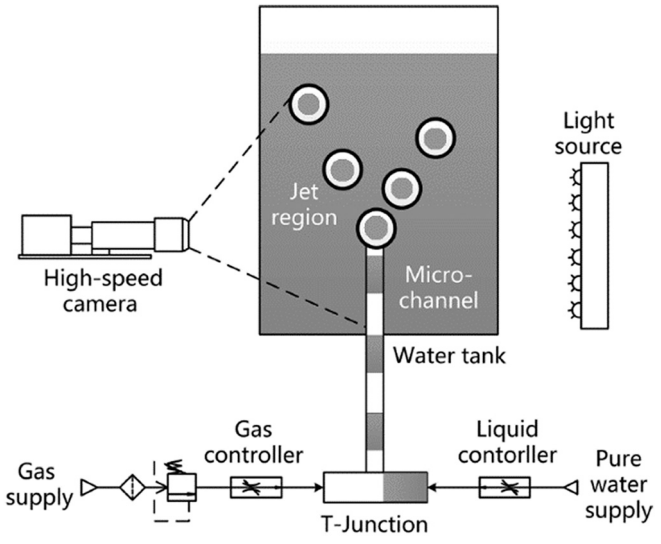

Fig. 8. Schematic representation of antibubble formation through Taylor flow [18,45].

2.5. Antibubble formation through submerged drop encapsulation

Recently, Shen and coworkers [18] reported antibubble formation through injection of Taylor flow into the bulk liquid (an aqueous solution with different glycerol concentrations) from the bottom. The Taylor flow was created through subsequent introduction of air and liquid slugs into a vertical microchannel through a T-junction. The mechanism of antibubble formation can be described as: i) formation of an air bubble that is detached by the following liquid slug, ii) penetration of liquid column into newly formed bubble to form liquid drop (Fig. 8).

The authors described the breakup of this short liquid column into a drop through radial necking and axial contraction, instead of classical Rayleigh-Plateau instability, which can be described by surface tension, viscosity and inertia, i.e., through Ohnesorge number, Oh (as defined in Section 2.3). For a sufficiently long liquid column (i.e., a high aspect ratio, $L_o = l/R$, where l and R are length and radius of liquid column), the droplet breakup is predominantly determined by the Ohnesorge number; whereas, for short liquid column length, the droplet breakup is also determined by the aspect ratio, as depicted in Fig. 9. In terms of surface tension effects, the relative onset of radial necking and axial contraction is quite important, which operate at different time scales at low and high Oh. Different forces operate below and above a critical Ohnesorge number, Oh_c, i.e., surface tension and viscous forces dominate when $Oh > Oh_c$, whereas, surface tension and inertial forces dominate when $Oh < Oh_c$. This gives a different value of characteristic time for the radial necking process.

2.6. Antibubble formation via particle stabilization

Pickering emulsions are surfactant-free dispersions that are stabilized by interfacial adsorption of solid particles. Such particle-laden interfaces usually offer exceptional stability against coalescence and Ostwald ripening as compared to surfactant-stabilized interfaces [46]. Additionally, various unusual dispersions such as W/W and O/O emulsions that are almost impossible to achieve via classical surfactants, can be produces via particle stabilization [47,48]. Interestingly, antibubbles were successfully produced by particle stabilization, which was initially introduced by Poortinga [19]. In this method, a liquid drop (containing maltodextrin and gelatin) was first coated with hydrophobized fumed silica particles. The particle-coated drop (termed as liquid marble) was gelled (by holding at 5 °C for 1 h) and then dropped into bulk liquid, also containing fumed silica particles (less hydrophobic than those present in

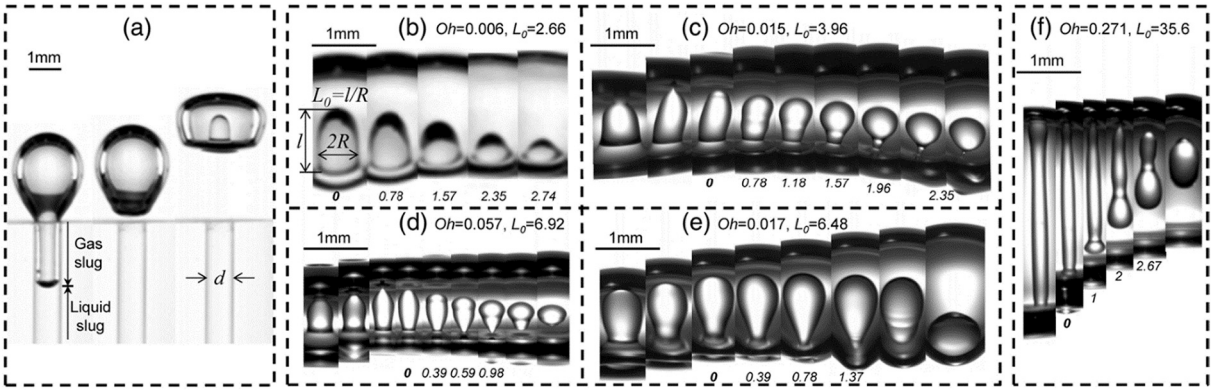

Fig. 9. Injection of Taylor flow into the liquid makes a liquid column penetrate a bubble; (b) the liquid column fails to break up with a small aspect ratio L_o; (c)–(f) at various Oh, the encapsulation structure is generated by the breakup process of a liquid column with a sufficiently large L_o [18].

the falling-drop). On impact with the bulk liquid, the falling coated-drop (liquid marble) entraps an air film and hence it ends into an antibubble (Fig. 10a). Principally, this process of antibubble formation is quite similar to the conventional method (discussed above), and the main difference is that the interfacial stabilization is achieved via particles (similar to Pickering emulsions). The role of maltodextrin is to achieve a higher density of the liquid marbles, which will facilitate their penetration into the bulk liquid (i.e., to counteract the buoyancy forces). Later on, the same author reported another method that was based on formation of a particle-stabilized W/O/W double emulsion [20]. For this, the inner as well as external aqueous phases of the double emulsion should contain a suitable solute (e.g., maltodextrin), whereas the middle phase should be a volatile oil (e.g., hexane). Similar to the method reported earlier [19], the stabilization of both interfaces is achieved by hydrophobized fumed silica particles. In this case, the particles were initially present in the middle oil phase and the outer aqueous phase used to prepare the double emulsion. The double Pickering emulsion can be prepared using conventional emulsification [20], or in a more controlled fashion such as through using a microfluidic system [49]. The freeze drying of this double emulsion transforms the aqueous phases into glassy state, and also removes the middle oil phase. Upon reconstitution in water, the maltodextrin will hydrate and the dried material will turn into an antibubbles dispersion, in which the inner aqueous phase is surrounded by a middle gaseous phase followed by the external aqueous (continuous) phase (Fig. 10b). Surprisingly, the core (i.e., inner glassy phase) gets rehydrated through adsorption of water vapors from the continuous phase, and the air shell remains intact through stabilization by the hydrophobic particles. It should be noted that as a double emulsion usually contains multiple water droplets inside the oil droplets, the antibubbles produced through this method may contain multiple liquid cores.

3. Stability of an antibubble - the role of surfactant and other factors

An antibubble is a thermodynamically unstable entity, which has an extremely short lifetime compared to other dispersed structures such as bubbles and droplets (Table 1). This is due to the surface tension, i.e., the collapse of an antibubble will result in a reduction of interfacial area and a release of interfacial energy, which is directly proportional to the surface tension. For instance, if we assume inner and outer diameters of an antibubble as 2 and 2.5 mm, respectively; one can calculate that after collapse, the interfacial area of the remaining gas bubble is reduced to 38% of the total antibubble interfacial area, thus reducing the interfacial energy. Furthermore, the thinner the air film relatively to the inner droplet volume, the more the reduction after collapse.

The lifetime of an antibubble is the time required by air (inside the air film) to move in upward direction under the action of hydrostatic pressure, i.e., the south pole (bottom) is at higher hydrostatic pressure than the north pole (top). This results in thinning of the air film towards

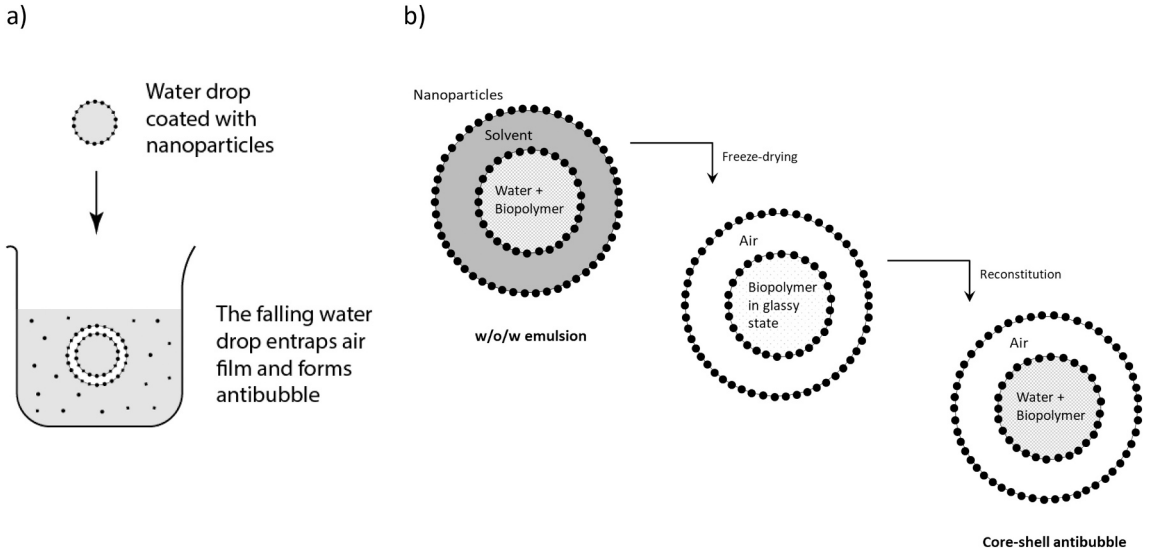

Fig. 10. A schematic representation of antibubble formation via particle stabilization: a) single drop method, b) double emulsion method.

the south pole, which ultimately leads to collapse of the antibubble [11]. Few earlier studies reported formation of antibubbles without surfactants, e.g., through using highly viscous liquids or oils [18,42]; however, the produced antibubbles indeed exhibited an extremely short lifetime (i.e., in the order of 100 millisecond). By using a suitable surfactant, antibubbles can be produced with a lifetime typically around few minutes. Principally, the surfactant molecules adsorbed at the air-liquid interface help in delaying air-film drainage of antibubbles – the main destabilization mechanism. Commercial detergents, and various ionic and non-ionic surfactants have been reported in different studies on antibubble formation (Table 1).

In spite of some similarities between antibubbles and bubbles, their lifetimes cannot be explained under the same argument due to a particular air-shell structure present in antibubbles. An air film is far less stable than a liquid film because of two major differences, as described by Dorbolo et al. [11]. Firstly, this can be explained through looking at the arrangement of surfactant molecules at the air-liquid interfaces of antibubbles and bubbles (Fig. 1). In ordinary bubbles thinning of the aqueous shell is opposed by electrostatic repulsion when charged surfactants are adsorbed at the interfaces. This repulsion stems from the overlap of the electric double layers. In the case of antibubbles stabilized by charged surfactants the electric double layers are present in the aqueous phases and not within the gaseous shell and hence this electrostatic repulsion is absent. Similarly, also steric repulsion forces that stabilize the gas film are absent because gas is a poor solvent. Therefore, the thinning of air-film proceeds upon drainage of the air film. Subsequently, Van der Waals interactions become significant between the interfaces of the air film, leading to destabilization of the whole system. The second basic factor that attributes to a greater stability of a bubble as compared to an antibubble is the effect of confinement [50]. The liquid films have a prominent Marangoni effect that opposes the drainage; whereas it is relatively less pronounced in air films as the surfactant molecules are present in the continuous phase, i.e., not in the film.

The interpretation of the role of surfactant in the lifetime of an antibubble is rather complex, compared to other dispersed structures. In other words, the lifetime of antibubble cannot be explained only in terms of peculiar surfactant properties, as properties of the liquid mixture are more important than merely the nature of surfactant used. For instance, it is difficult to obtain an antibubble with a solution of surfactant only, and therefore, glycerol is often added into the liquid mixture to get a higher probability of antibubble formation [11]. This requires a better understanding of interfacial rheology of the liquid mixture. Initially, it was found experimentally that the surface viscoelastic moduli of the liquid mixtures play a crucial role in the lifetime of the antibubble through determining the type of air flow during the air-film drainage [11]. That is, the air film drainage proceeds either more *Poiseuille-like* or *plug* flow depending upon if the surface modulus is high or low, respectively. A longer lifetime was related to Poiseuille flow due to a slow air-film drainage. They reported that the mean antibubble lifetime can be doubled by increasing the surface modulus by a factor 100. Furthermore, Scheid et al. [7] proposed a theoretical model based on the lubrication theory for air-film drainage to describe the role of surface shear viscosity on the lifetime of antibubbles. Their theoretical and experimental observations reflected that the lifetime of antibubbles increases with surface shear viscosity. One of the assumptions of their model was that the adsorption kinetic of surfactant molecules is much faster than the lifetime of antibubble, i.e., the surface tension gradients that arise due to air-film drainage are balanced by a fast adsorption of surfactants at the interface. However, this assumption is not compatible with all surfactants, e.g., hexaethylene glycol monododecyl ether ($C_{12}E_6$), which has comparatively lower adsorption rate [51] and an extremely small surface shear viscosity [52], can produce antibubbles with lifetime nearly equal to its adsorption rate [6]. Therefore, Vitry el al. [13] recently elaborated the role of surface elasticity as the most decisive factor in controlling the lifetime of antibubbles. A higher surface elasticity favors a longer lifetime through the onset of Marangoni stresses (in response to depletion of surfactant molecules from interface) at the south pole that counters the air-film drainage. A detailed information on surfactant dynamics including Marangoni stresses at fluid interfaces can be found elsewhere [53]. During air-film drainage in an antibubble, the Marangoni stresses operate until the surfactant concentration gradients are minimized through adsorption of surfactant from the liquid phases. Ultimately, the air film reaches to a critically low value and destabilized by van der Walls interactions as discussed above. Vitry el al. [13] reported a threshold value of 0.03 for the Marangoni number (Ma_{th}) – a characteristic for surface rigidity (comparing the surface elasticity to the hydrostatic pressure force), above which the lifetime becomes nearly independent of surface elasticity, but then depends on surfactant concentration in the bulk.

The discussion so far attributes instability of an antibubble due to air flow (or drainage) from bottom to top of the antibubble. However, another stabilization could also arise due to dissolution or loss of gas into the bulk liquid [12,13]. This happens as the gas-liquid interface is permeable and allows exchange of gases through it. This is even true if the interface is fully covered with, e.g. water-soluble, surfactants [54], which is usually the case with antibubbles. Therefore, the air content of bulk liquid can significantly affect the lifetime of antibubble, i.e., a longer lifetime if the liquid is saturated with gas, and vice versa. Nevertheless, the mass transfer coefficient through the interface can vary in response to some physical factors such as liquid flow with respect to the interface (e.g., when antibubble is rising due to density difference), temperature, etc.

The stability of antibubbles may be impacted by some other factors such as size of the antibubble, air film thickness (as mathematically explained at the beginning of this section), and quality of the entrapped air, which are briefly discussed here (based on experimental findings as reported in literature). Initially, it was believed that the lifetime is independent of antibubble size [6,9]; however later Vitry et al. [13] reported a significant influence of radius on antibubble lifetime. In spite of a large dispersion in their experimental values, there was a clear trend showing an increase in lifetime as a function of radius (in the range of 0.5–2.5 mm), which was also consistent with their numerical model. They further elaborated the effect of antibubble radius in relation to surface elasticity, i.e. as long as the interfacial surface is sufficiently elastic and rigid (i.e., $Ma_{th} > 0.3$, as mentioned above) the larger antibubbles would have a longer life expectancy. However, for a given surface elasticity, there is a radius above which the Marangoni stresses ultimately becomes insufficient to counteract air-film drainage.

Another closely related parameter regarding production of antibubble is the air-film thickness. The air-liquid interface usually undergoes regular deformations due to surface waves that are produced by impacting liquid drop/jet. This results in variability in the way the liquid jet/drop impinges the air-liquid interface, which in turn may result in variation in initial air-film thickness among consecutively produced antibubbles [13]. As an antibubble is destabilized due to upward movement of the entrapped air, so one might get an impression that a higher initial air-film thickness could result in a longer antibubble lifetime. However, in reality this is not true, as experimentally established by Vitry et al. [13] who observed lifetimes of 130 rising antibubbles having different initial air-film thicknesses (the mean value was typically around 4.0 $\pm$ 1.3 μm). Similar finding was also reported by Kim and Vogel [9], i.e., the air drainage time is independent of the air-film thickness. This supports the theory of a heterogenous air-film drainage due to existence of air channels, i.e., a variable thickness along the antibubble latitude [6]. However, contrary to air-film thickness, the quality of entrapped air can significantly impact antibubble lifetime. For instance, dust particles or any contamination can significantly destabilize antibubbles, either by altering the surface tension or by interfering with air-film to initiate an early rupture [9,13]. Vitry et al. [13] reported that 0.3 μm dust particle can definitely destabilize 0.5 μm thick air-shell with an assumption that the long-range intermolecular forces of about

100 nm are responsible for the rupture. Moreover, the large sized antibubbles were found more vulnerable to dust particles in comparison to smaller ones, due to existence of large air volumes in the former case and hence a larger chance that dust particles are entrapped inside the air film.

Since the cause of instability of antibubbles is generally the air-film drainage under the influence of gravity, the lifetime of antibubbles can be prolonged by movement of the antibubbles in such a way that the gas film has no time to drain. In the study of Shen et al. [18], this was achieved through application of shear flow on antibubbles. Even in case of severe deformation of the antibubble due to strong shear flow, the outer air-shell and inner liquid-drop was found rather stable against breakage and coalescence, respectively, until a shear rate of 602/s. However, a more practical approach to ensure extended lifetime is through particle-based stabilization of antibubbles, as discussed in Section 2.6. The lifetime in this case could be around at least hours (Table 1), which is much longer than that of surfactant-stabilized antibubbles. In case of Pickering emulsions, the colloidal particles are adsorbed irreversibly at the liquid-liquid interface, and can form a tightly packed layer of particles around the drops. This provides a better resistance against coalescence, and therefore Pickering emulsions are believed to have much higher stability as compared to emulsions stabilized by surfactants [55]. Particle-stabilized antibubbles can be considered analogous to liquid marbles floating on water [56]. A liquid marble can be formed by coating of a liquid drop with micro- or nanoparticles. A liquid marble floating on a bulk liquid surface, e.g., water, is separated by a thin air film from the liquid below and can be destabilized due to bursting (when particles covering the liquid marble are transferred to the supporting liquid surface) or shrinkage (due to evaporation) [57]. The particle size, surface free energy and hydrophobicity of the encapsulating microparticles determine the effective surface tension and lifetime of a liquid marble floating on water [58]. Although, the destabilization mechanism for a liquid marble is different than that of an antibubble, however, the available literature on liquid marbles can be extrapolated to antibubbles. Still further investigations are needed to find the exact destabilization mechanism for particle-stabilized antibubbles.

4. Potential applications of an antibubble

Encapsulation technology has witnessed an unprecedent development in the past two decades as evident from multiple applications in food, pharmaceutical and chemical industries [59–61]. A number of encapsulation strategies are currently available, producing encapsulation matrices all the way down to the nanoscale; however, each with distinct pros and cons. An antibubble is one such strategy, yet an entirely different approach, in which an air shell is used to encapsulate an inner liquid core (that may contain the active component to be delivered). This specific structure of an antibubble makes it an attractive system which could offer innovative applications, entirely different from existing encapsulation strategies. For instance, they may promise a more precise delivery and a site-specific release of the active components in response to external fields such as ultrasound [17] and magnetic fields [21]. In medical imaging, microbubbles are already being applied as ultrasound contrast agents (UCA) to locate pathological tissues [62]. In the past, efforts have been carried out to load and deliver bioactive components through acoustically active microspheres having thick lipid shells [63,64]. However, such microspheres need high acoustic amplitude to release the loaded material due to a high viscoelasticity of the lipid shell [65]. Therefore, antibubbles could serve as potential UCA along with delivery of a therapeutic component to a specific area inside the body. The susceptibility of antibubbles towards ultrasound can be tuned by regulating the core size that would make them suitable vehicles in ultrasonic imaging and ultrasound-guided drug delivery [65,66]. It should be noted here that in their work Postema et al. [66] extended the antibubble concept to bubbles containing solid instead of liquid cores. Furthermore, the delivery of antibubbles can be regulated through application of external magnetic fields, as reported by Silpe and McGrail [21]. Such magnetic antibubbles can be produced through dispersion of iron oxide (Fe_3O_4) microparticles in the liquid core, while their flow can be controlled through regulating factors such as Fe_3O_4 concentration, magnetic field strength and other fluid properties of the system. However, these investigations are mostly conceptional, as no real application has been reported to date. This is primarily due to the extremely short lifetime of surfactant-stabilized antibubbles. In that respect, the core-shell or particle-stabilized antibubbles seem an attractive alternative to conventional antibubbles. For instance, in a recent study [67] such core-shell antibubbles are reported for the encapsulation of probiotics (i.e., *Lactobacillus casei*) to protect them from external environment. The researchers found an improved viability of these bacteria after 1 h of incubation at low pH (analogous to gastric conditions). A further research in this regard could focus on achieving high encapsulation efficiencies, and also on studying controlled release behavior of the core material, e.g., through change in wettability of particles in time or in response of any external stimuli. Here, it is important to realize that if the goal is to generate small antibubbles, i.e., down to (sub)micron scale, then we may have to rely on surfactant-based stabilization. This warrants further study of the possibilities to stabilize antibubbles using surfactants.

5. Conclusions

Several techniques can be employed for the preparation of antibubbles, in which the creation of an air-film around a liquid drop can be realized either through surface entrapment (e.g., via impact of a falling jet/drop on a bulk liquid), submerged drop encapsulation (e.g., via a submerged capillary carrying a Taylor flow), or through evaporation of a volatile oil phase (e.g., in case of particle stabilized W/O/W emulsion). The antibubble in each of these techniques is produced by a distinct mechanism, through a careful optimization of the related process parameters. Another logical basis of classification of antibubble formation could be based on the stabilization mechanism, i.e., i) surfactant stabilized, and ii) particle stabilized. The majority of studies reported so far, were based on surfactant stabilization. However, a complete understanding of how surfactants facilitate antibubble formation and stabilize antibubbles is lacking. The researchers are still unable to produce small (preferably less than 100 μm) stable surfactant-stabilized antibubbles. Hence, a short lifetime of surfactant-stabilized antibubbles is still a major issue that is hindering their potential applications. Therefore, the particle-based stabilization seems a promising approach, which can produce antibubbles with long-term stability. This can finally enable us to achieve a range of envisaged applications of antibubbles. However, our understanding of when such particle-stabilized antibubbles burst is still incomplete and further research on this is required to obtain antibubbles with controlled release behavior. This will generate the knowledge to for example build antibubbles that become unstable at low pH such as in the stomach or in the vicinity of a tumor. Similarly, different applications will require different stabilizing systems sensitive to specific triggers. To achieve this, much research is still needed.

Declaration of Competing Interest

The authors declare that they have no known competing financial interests or personal relationships that could have appeared to influence the work reported in this paper.

References

[1] Hughes W, Hughes AR. Liquid drops on the same liquid surface. Nat 1932. https://doi.org/10.1038/129059a0. 1293245 1932;129:59–59.
[2] Skogen N. Inverted soap bubbles—a surface phenomenon. Am J Physiol 1956;24:239–41. https://doi.org/10.1119/1.1934198.
[3] Baird MHI. The stability of inverse bubbles. Trans Faraday Soc 1960;56:213–9. https://doi.org/10.1039/TF9605600213.
[4] Stong C. The amateur scientist: curious bubbles in which a gas encloses a liquid instead of the other way around. Sci Am 1974;230.
[5] Dorbolo S, Caps H, Vandewalle N. Fluid instabilities in the birth and death of antibubbles. New J Phys 2003;5. https://doi.org/10.1088/1367-2630/5/1/161.
[6] Dorbolo S, Reyssat E, Vandewalle N, Quéré D. Aging of an antibubble. Europhys Lett 2005;69:966–70. https://doi.org/10.1209/epl/i2004-10435-7.
[7] Scheid B, Dorbolo S, Arriaga LR, Rio E. Antibubble dynamics: the drainage of an air film with viscous interfaces. Phys Rev Lett 2012;109:1–5. https://doi.org/10.1103/PhysRevLett.109.264502.
[8] Sob'yanin DN. Theory of the antibubble collapse. Phys Rev Lett 2015;114:1–5. https://doi.org/10.1103/PhysRevLett.114.104501.
[9] Kim PG, Vogel J. Antibubbles: factors that affect their stability. Colloids Surfaces A Physicochem Eng Asp 2006;289:237–44. https://doi.org/10.1016/j.colsurfa.2006.04.048.
[10] Kim PG, Stone HA. Dynamics of the formation of antibubbles. Epl 2008;83. https://doi.org/10.1209/0295-5075/83/54001.
[11] Dorbolo S, Terwagne D, Delhalle R, Dujardin J, Huet N, Vandewalle N, et al. Antibubble lifetime: influence of the bulk viscosity and of the surface modulus of the mixture. Colloids Surfaces A Physicochem Eng Asp 2010;365:43–5. https://doi.org/10.1016/j.colsurfa.2010.01.028.
[12] Scheid B, Zawala J, Dorbolo S. Gas dissolution in antibubble dynamics. Soft Matter 2014;10:7096–102. https://doi.org/10.1039/C4SM00718B.
[13] Vitry Y, Dorbolo S, Vermant J, Scheid B. Controlling the lifetime of antibubbles. Adv Colloid Interface Sci 2019;270:73–86. https://doi.org/10.1016/j.cis.2019.05.007.
[14] Bai L, Xu W, Wu P, Lin W, Li C, Xu D. Formation of antibubbles and multilayer antibubbles. Colloids Surfaces A Physicochem Eng Asp 2016;509:334–40. https://doi.org/10.1016/j.colsurfa.2016.09.032.
[15] Song Y, Zhang L, Wang EN. Criteria for antibubble formation from drop pairs impinging on a free surface. Phys Rev Fluids 2020;5:123601. https://doi.org/10.1103/PhysRevFluids.5.123601.
[16] Tufaile A, Sartorelli JC. Bubble and spherical air shell formation dynamics. Phys Rev E - Stat Physics, Plasmas, Fluids, Relat Interdiscip Top 2002;66:7. https://doi.org/10.1103/PhysRevE.66.056204.
[17] Postema M, ten Cate F, Schmitz G, de Jong N, van Wamel A. Generation of a droplet inside a microbubble with the aid of an ultrasound contrast agent: first result. Lett Drug Des Discov 2007;4:74–7. https://doi.org/10.2174/157018007778992847.
[18] Shen Y, Hu L, Chen W, Xie H, Fu X. Drop encapsulated in bubble: a new encapsulation structure. Phys Rev Lett 2018;120:54503. https://doi.org/10.1103/PhysRevLett.120.054503.
[19] Poortinga AT. Long-lived antibubbles: stable antibubbles through Pickering stabilization. Langmuir 2011;27:2138–41. https://doi.org/10.1021/la1048419.
[20] Poortinga AT. Micron-sized antibubbles with tunable stability. Colloids Surfaces A Physicochem Eng Asp 2013;419:15–20. https://doi.org/10.1016/j.colsurfa.2012.11.040.
[21] Silpe JE, McGrail DW. Magnetic antibubbles: formation and control of magnetic macroemulsions for fluid transport applications. J Appl Phys 2013;113. https://doi.org/10.1063/1.4796147.
[22] Hsiao M, Lichter S, Quintero LG. The critical weber number for vortex and jet formation for drops impinging on a liquid pool. Phys Fluids 1988;31:3560. https://doi.org/10.1063/1.866872.
[23] Elmore PA. The entrainment of bubbles by drop impacts. J Fluid Mech 1990;220:539–67. https://doi.org/10.1017/S0022112090003378.
[24] Yakhshi-Tafti E, Cho HJ, Kumar R. Impact of drops on the surface of immiscible liquids. J Colloid Interface Sci 2010;350:373–6. https://doi.org/10.1016/J.JCIS.2010.06.029.
[25] Marston JO, Thoroddsen ST. Apex jets from impacting drops. J Fluid Mech 2008;614:293–302. https://doi.org/10.1017/S0022112008003881.
[26] Deng Q, Anilkumar AV, Wang TG. The role of viscosity and surface tension in bubble entrapment during drop impact onto a deep liquid pool. J Fluid Mech 2007;578:119–38. https://doi.org/10.1017/S0022112007004892.
[27] Okawa T, Shiraishi T, Mori T. Production of secondary drops during the single water drop impact onto a plane water surface. Exp Fluids 2006;41:965–74. https://doi.org/10.1007/S00348-006-0214-X.
[28] Thoroddsen ST, Etoh TG, Takehara K. Air entrapment under an impacting drop. J Fluid Mech 2003:125–34. https://doi.org/10.1017/S0022112002003427.
[29] Rein M. Phenomena of liquid drop impact on solid and liquid surfaces. Fluid Dyn Res 1993;12:61–93. https://doi.org/10.1016/0169-5983(93)90106-K.
[30] Weiss DA, Yarin AL. Single drop impact onto liquid films: neck distortion, jetting, tiny bubble entrainment, and crown formation. J Fluid Mech 1999;385:229–54. https://doi.org/10.1017/S002211209800411X.
[31] Manzello SL, Yang JC. An experimental study of a water droplet impinging on a liquid surface. Exp Fluids 2002;32:580–9. https://doi.org/10.1007/S00348-001-0401-8.
[32] Yarin AL. Drop impact dynamics: splashing, spreading, receding, bouncing. Annu Rev Fluid Mech 2006;38:159–92. https://doi.org/10.1146/ANNUREV.FLUID.38.050304.092144.
[33] Deka H, Ray B, Biswas G, Dalal A, Tsai PH, Wang AB. The regime of large bubble entrapment during a single drop impact on a liquid pool. Phys Fluids 2017;29. https://doi.org/10.1063/1.4992124.
[34] Terwagne D. Bouncing droplets, the role of deformations. 2011.
[35] Nakai T, Ueno T, Kanzawa K, Goto T. Temperature dependence of the lifetime of a droplet on a liquid surface. J Robot Mechatron 2011;23:386–92. https://doi.org/10.20965/JRM.2011.P0386.
[36] Zou J, Wang PF, Zhang TR, Fu X, Ruan X. Experimental study of a drop bouncing on a liquid surface. Phys Fluids 2011;23:044101. https://doi.org/10.1063/1.3575298.
[37] Michon GJ, Josserand C, Séon T. Jet dynamics post drop impact on a deep pool. Phys Rev Fluids 2017;2:023601. https://doi.org/10.1103/PHYSREVFLUIDS.2.023601/FIGURES/7/MEDIUM.
[38] Richard D, Clanet C, Quéré D. Surface phenomena: contact time of a bouncing drop. Nature 2002;417:811. https://doi.org/10.1038/417811A.
[39] Couder Y, Fort E, Gautier CH, Boudaoud A. From bouncing to floating: noncoalescence of drops on a fluid bath. Phys Rev Lett 2005;94:177801. https://doi.org/10.1103/physrevlett.94.177801.
[40] Amarouchene Y, Cristobal G, Kellay H. Noncoalescing drops. Phys Rev Lett 2001;87:206104–1–206104–4. https://doi.org/10.1103/PhysRevLett.87.206104.
[41] Wang W, Lin F, Wei X, Zou J. Antibubble formation by a single drop impact on a free surface. Phys Fluids 2021;33:042107. https://doi.org/10.1063/5.0047598.
[42] Beilharz D, Guyon A, Li EQ, Thoraval MJ, Thoroddsen ST. Antibubbles and fine cylindrical sheets of air. J Fluid Mech 2015;779:87–115. https://doi.org/10.1017/jfm.2015.335.
[43] Zhao H, Brunsvold A, Munkejord ST. Investigation of droplets impinging on a deep pool: transition from coalescence to jetting. Exp Fluids 2010 503 2010;50:621–35. doi:https://doi.org/10.1007/S00348-010-0966-1.
[44] Zhao H, Brunsvold A, Munkejord ST. Transition between coalescence and bouncing of droplets on a deep liquid pool. Int J Multiph Flow 2011;37:1109–19. https://doi.org/10.1016/J.IJMULTIPHASEFLOW.2011.06.007.
[45] Shen Y, Hu L, Chen W, Fu X. Periodic and aperiodic bubbling in submerged gas-liquid jets through a micro-channel. Phys Fluids 2017;29. https://doi.org/10.1063/1.4979483.
[46] Tai Z, Huang Y, Zhu Q, Wu W, Yi T, Chen Z, et al. Utility of Pickering emulsions in improved oral drug delivery. Drug Discov Today 2020;25:2038–45. https://doi.org/10.1016/j.drudis.2020.09.012.
[47] Nicolai T, Murray B. Particle stabilized water in water emulsions. Food Hydrocoll 2017;68:157–63. https://doi.org/10.1016/j.foodhyd.2016.08.036.
[48] Binks BP, Tyowua AT. Oil-in-oil emulsions stabilised solely by solid particles. Soft Matter 2016;12:876–87. https://doi.org/10.1039/C5SM02438B.
[49] Silpe JE, Nunes JK, Poortinga AT, Stone HA. Generation of antibubbles from core-shell double emulsion templates produced by microfluidics. Langmuir 2013;29:8782–7. https://doi.org/10.1021/la4009015.
[50] Delacotte J, Montel L, Restagno F, Scheid B, Dollet B, Stone HA, et al. Plate coating: influence of concentrated surfactants on the film thickness. Langmuir 2012;28:3821–30. https://doi.org/10.1021/LA204386B.
[51] Lin SY, Lee YC, Shao MM. Adsorption kinetics of C12E6 at the air-water interface. J Chinese Inst Chem Eng 2002;33:631–43.
[52] Zell ZA, Nowbahar A, Mansard V, Leal LG, Deshmukh SS, Mecca JM, et al. Surface shear inviscidity of soluble surfactants. Proc Natl Acad Sci 2014;111:3677–82. https://doi.org/10.1073/PNAS.1315991111.
[53] Manikantan H, Squires TM. Surfactant dynamics: hidden variables controlling fluid flows. J Fluid Mech 2020;892:1. https://doi.org/10.1017/JFM.2020.170.
[54] Hanwright J, Zhou J, Evans GM, Galvin KP. Influence of surfactant on gas bubble stability. Langmuir 2005;21:4912–20. https://doi.org/10.1021/LA0502894.
[55] Gonzalez Ortiz D, Pochat-Bohatier C, Cambedouzou J, Bechelany M, Miele P. Current trends in Pickering emulsions: particle morphology and applications. Engineering 2020;6:468–82. https://doi.org/10.1016/J.ENG.2019.08.017.
[56] Aussillous P, Quéré D. Liquid marbles. Nat 2001;4116840 2001(411):924–7. https://doi.org/10.1038/35082026.
[57] Fujii S, Kameyama S, Armes SP, Dupin D, Suzaki M, Nakamura Y. pH-responsive liquid marbles stabilized with poly(2-vinylpyridine) particles. Soft Matter 2010;6:635–40. https://doi.org/10.1039/B914997J.
[58] Cengiz U, Erbil HY. The lifetime of floating liquid marbles: the influence of particle size and effective surface tension. Soft Matter 2013;9:8980–91. https://doi.org/10.1039/c3sm51304a.
[59] Tylkowski B, Giamberini M, Fernandez Prieto S. Microencapsulation. 2nd ed. Berlin: De Gruyter; 2020. https://doi.org/10.1515/9783110642070.
[60] Mishra M. Handbook of encapsulation and controlled release. CRC press; 2015.
[61] Sonawane S, Bhanvase B, Sivakumar M. Encapsulation of active molecules and their delivery system. Elsevier; 2020.
[62] Frinking P, Segers T, Luan Y, Tranquart F. Three decades of ultrasound contrast agents: a review of the past, present and future improvements. Ultrasound Med Biol 2020;46:892–908. https://doi.org/10.1016/J.ULTRASMEDBIO.2019.12.008.

[63] May DJ, Allen JS, Ferrara KW. Dynamics and fragmentation of thick-shelled microbubbles. IEEE Trans Ultrason Ferroelectr Freq Control 2002;49:1400–10. https://doi.org/10.1109/TUFFC.2002.1041081.
[64] Shortencarier MJ, Dayton PA, Bloch SH, Schumann PA, Matsunaga TO, Ferrara KW. A method for radiation-force localized drug delivery using gas-filled lipospheres. IEEE Trans Ultrason Ferroelectr Freq Control 2004;51:822–31. https://doi.org/10.1109/TUFFC.2004.1320741.
[65] Kotopoulis S, Johansen K, Gilja OH, Poortinga AT, Postema M. Acoustically active antibubbles. Acta Phys Pol A 2015;127:99–102. https://doi.org/10.12693/APhysPolA.127.99.
[66] Postema M, Novell A, Sennoga C, Poortinga AT, Bouakaz A. Harmonic response from microscopic antibubbles. Appl Acoust 2018;137:148–50. https://doi.org/10.1016/j.apacoust.2018.03.021.
[67] Mardani Ghahfarokhi V, Pescarmona PP, Euverink G-JW, Poortinga AT. Encapsulation of *lactobacillus casei* (ATCC 393) by Pickering-stabilized antibubbles as a new method to protect bacteria against low pH. Colloids Interf 2020;4:40. https://doi.org/10.3390/colloids4030040.
[68] Dorbolo S, Vandewalle N. Antibubbles: Evidences of a critical pressure. 2003.